

# Miscibility study of Torlon® polyamide-imide with Matrimid® 5218 polyimide and polybenzimidazole

Yan Wang <sup>a</sup>, Suat Hong Goh <sup>a</sup>, Tai-Shung Chung <sup>b,\*</sup>

<sup>a</sup> Department of Chemistry, National University of Singapore, 3 Science Drive 3, Singapore 117543, Singapore

<sup>b</sup> Department of Chemical and Environmental Engineering, National University of Singapore, 10 Kent Ridge Crescent, Singapore 119260, Singapore

Received 2 November 2006; received in revised form 9 March 2007; accepted 15 March 2007

Available online 19 March 2007

## Abstract

We have discovered two new miscible polymer blend systems, namely, Torlon® 4000T with Matrimid® 5218 and Torlon 4000T with polybenzimidazole (PBI). Both Matrimid 5218 and PBI are miscible at a molecular level with Torlon 4000T over the whole composition range as confirmed by microscopy, DSC, FTIR and DMA. DSC and DMA studies show the existence of a single glass transition in each blend. The  $T_g$ -composition curve of Torlon/Matrimid blend system forms a sigmoid curve as a function of composition, while the  $T_g$ -composition curve of the Torlon/PBI blend system is double parabola-like. FTIR spectra show the existence of hydrogen-bonding interactions in these two polymer blend systems.

© 2007 Elsevier Ltd. All rights reserved.

**Keywords:** Torlon; Miscible polymer blend;  $T_g$ -composition curve

## 1. Introduction

Polyamide-imides (PAIs) have been commercially available for several decades. Their synthesis, properties and applications have been extensively described along with those of polyamides and polyimides. Their superior mechanical, thermal and oxidative properties have made them suitable for various applications in industrial processes, transportation, and electrical equipment. Torlon® 4000T PAI, developed recently by Solvay Advanced Polymer as one of the Torlon 4000 series, is an unfilled PAI powder for adhesive applications according to Ref. [1]. The chemical structure of Torlon 4000T PAI, which has been investigated by Robertson et al. [2] using NMR spectroscopy, is shown in the Fig. 1.

Since Torlon 4000T is a relatively new commercial polymer, there are limited studies on this material. Till now there are only three blend systems involving Torlon are mentioned in literature. Gelatin/Torlon 4000T membranes were used by Yoshikawa et al. for the vapor permeation of aqueous

2-propanol solutions [3] and their result showed that the blend membrane gives a much better performance than the neat Torlon film [4,5]. The blend system was supposed to be miscible because the films were transparent and homogeneous. However, there was no investigation on the miscibility and interactions of this polymer blend system. Other blend systems of Torlon are Torlon/SPEEK (sulfonated poly(ether ether ketone)) and Torlon/SAPEEK (sulfamidated poly(ether ether ketone)), reported by Karcha and Porter [6–8]. Blends of PEEK with Torlon were reported to be immiscible, but SPEEK and SAPEEK were found to be miscible at all compositions with Torlon 4000T. The third blend system involving Torlon is the Torlon 4203L (measured  $T_g = 293$  °C)/PEI (Ultem 1000) system reported by Palsule and Cowie [9].

In this paper, we report two new miscible polymer blend systems, namely, Torlon with Matrimid® 5218 polyimide, and Torlon with polybenzimidazole (PBI). Miscibility was observed over the whole composition range, as indicated by the transparency of the films and the existence of a single glass transition in each blend.

PBI is a glassy polymer with high  $T_g$ , outstanding thermal stability and chemical resistance. PBI has been developed for

\* Corresponding author. Tel.: +65 6516 6645; fax: +65 6779 1936.

E-mail address: [chents@nus.edu.sg](mailto:chents@nus.edu.sg) (T.-S. Chung).

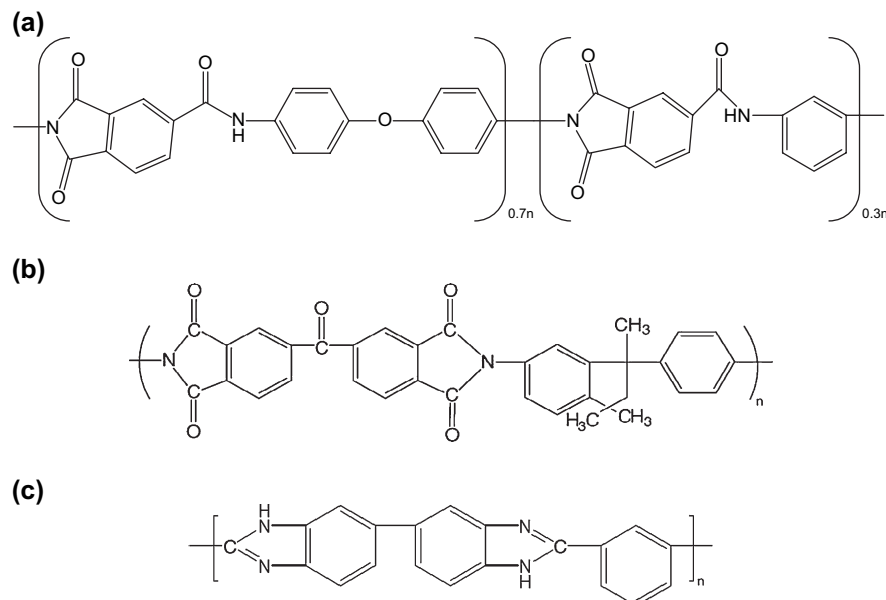


Fig. 1. Chemical structures of polymers: (a) Torlon® 4000T polyamide-imide, (b) Matrimid® 5218, and (c) polybenzimidazole.

reverse osmosis and microporous membranes and recently as membrane separators for fuel cells because of its superior stability in high-temperature corrosive environments. The use of polybenzimidazole (PBI) doped with phosphoric acid as an electrolyte in intermediate temperature fuel cells (150–200 °C) and hydrogen sensors [10–12] has received a lot of attention recently since it exhibited excellent thermal stability and high proton conductivity even at anhydrous state. However, the commercial PBI, which has the structure as shown in Fig. 1, is very brittle for the fabrication of self-standing membranes.

Blending may be a good way to overcome its shortcomings and synergistically combine the advantages of the individual components. PBI possesses both donor and acceptor hydrogen-bonding sites, which are capable of participating in specific interactions and thus favorable to form miscible blends with some other polymers. Blending offers the opportunity to extend the application range of these materials into the area of functional polymers. The enhanced proton conductivity of phosphoric acid doped PBI blends is one of many examples [12–14].

Blends of PBI and several polyimides have been widely investigated in recent years and it was claimed that miscibility occurred for some composition range or over a wide composition range [15–22]. Studies also revealed phase separation upon annealing, and the phase behavior of the systems was found to be dependent both on the type of polyimide and on thermal history. Hydrogen-bonding interactions between carbonyl groups in polyimides and NH groups in PBI were believed to be responsible for the miscibility. Since Torlon has an imide structure in its polymer chains, hydrogen bonding could also take place between the carbonyl group on polyimide structure of Torlon and NH group in PBI.

PI/PI blends have also been extensively studied [9,23–31]. It is generally considered that there are charge transfer interactions between the benzene rings of the phthalimides and the

benzene ring in the diamine units or between the imide group and the *p*-phenylene group of PIs that accounts for the miscibility of the two PI polymers [23,24,31]. Matrimid 5218 is a commercially available polyimide from Ciba Specialty Chemicals Ltd. and is one of the most popular polyimide materials for gas separation studies and chemical modifications [32–47] because of its high glass transition temperature ( $T_g$ ), good processability and superior combination in selectivity and permeability. We have found that it shows good performance in gas separation and pervaporation [39–47]. However, its low anti-plasticization characteristics [36,40,41] and extremely high cost limit its wide usage. Blending with Torlon may provide a possibility to enhance its anti-plasticization resistance and decrease its cost reasonably without compromising the good performance. The polyimide, Matrimid has been reported to be miscible with other polyimides such as P84 [29] and PEI [48,49] on a molecular level.

## 2. Experimental

### 2.1. Materials

Torlon 4000T was supplied by Solvay Advanced Polymers. Matrimid 5218 (3,3',4,4'-benzophenone tetracarboxylic dianhydride and diamino-phenylindane) powder was supplied by Ciba Polymers (Hawthorne, New York). PBI powder was purchased from Aldrich Chemical Company. All polymers were dried overnight at 120 °C under vacuum before use. *N,N*-Dimethylformamide (DMF) was employed as the solvent to prepare dense films of the polymer blends. It was supplied by Fisher Scientific with analytical grade and used as received.

### 2.2. Preparation of polymer blends

Thick films (40–60  $\mu\text{m}$ ) were cast from 2 wt% DMF solutions of polymer mixtures of varying compositions on Teflon

petri dishes at 55 °C for 3–4 days, due to the high boiling point of DMF. The resultant films were further dried under vacuum with temperature gradually increased to 250 °C and held there for at least 1–2 days to remove residual solvent. The resulted films are transparent and homogeneous in their dried state, suggesting that they may be miscible.

### 2.3. Morphology observation

The surface morphology of the blend film was observed by a polarized light microscope (PLM) (Olympus BX 50) with crossed polarizers between which a red plate having the retardation of 530 nm was inserted. The data of the micrographs were analyzed by an imaging software (Image-Pro Plus 3.0).

To observe the images at higher magnifications, the surface morphology of the blend film and the fracture surface of the dense films were also observed using a JSM-6700F field emission scanning electron microscope (FESEM). Samples were fractured after immersion in liquid nitrogen for a few minutes to reduce damage to the morphology. The prepared surfaces were sputter coated with platinum to provide enhanced conductivity.

### 2.4. Differential scanning calorimetry (DSC)

The  $T_g$ s of various polymers and blends were measured with a Perkin–Elmer Pyris-1 differential scanning calorimeter using a heating rate of 20 °C/min. Sample sizes range from 7 to 15 mg. The  $T_g$  value is taken as the middle of the slope transition in the DSC curve. The reported  $T_g$  value is the average value based on the second runs of at least three samples. To study the possible effect of annealing on phase behavior, each sample was brought to a desired annealing temperature in the DSC and annealed for 10 min, followed by quenching to 50 °C at a heating rate of 90 °C/min. The samples were rescanned up to 400 °C for Torlon/Matrimid blends and 450 °C for Torlon/PBI blends.

### 2.5. Modulated differential scanning calorimetry (MDSC)

The samples were also examined with a TA Instrument 2920 modulated differential scanning calorimeter (MDSC), using a heating rate of 3 °C/min with an oscillation amplitude

of  $\pm 0.65$  °C with an oscillation period of 45 s. This ideal heating rate is suggested to be the one that will provide a minimum of four temperature oscillations over the temperature range of the transition.

### 2.6. Fourier transform infrared spectroscopy (FTIR)

Samples for infrared spectroscopic analysis were prepared by casting a film onto a KBr disc from a 2% (w/w) solution in DMF. Solvent was first allowed to evaporate at 55 °C for 3–4 days. The cast films attached on the KBr discs were later dried under vacuum at 100 °C for 1 week. Infrared spectra were obtained on a Perkin–Elmer FTIR Spectrum 2000 with a resolution of 2  $\text{cm}^{-1}$ . The spectra were obtained with an average of 32 scans. The film used in this study was sufficiently thin to be within an absorbance range where the Beer–Lambert's law is obeyed.

### 2.7. Dynamic mechanical analysis (DMA)

The dynamic mechanical analysis was performed with DMA2980 from TA Instruments at a heating rate of 3 °C/min from room temperature to 450 °C and a frequency of 1 Hz. The storage modulus, loss modulus and  $\tan \delta$  changes of the dense film, under oscillating load, were monitored against time, temperature or frequency of oscillation in the above specified temperature range.

## 3. Results and discussion

### 3.1. Morphology of the blend films

Fig. 2 shows the PLM images of the dense film surfaces of Torlon/Matrimid and Torlon/PBI blend systems. The images are both clear and homogeneous, indicating the miscibility of the two blend systems.

FESEM micrographs in Figs. 3 and 4 show the top surfaces and the fracture surfaces of the dense films of the two polymer blends of different compositions at a much higher magnification. The FESEM micrographs show that generally the morphology is rough and homogeneous. The two polymers are homogeneously mixed. Each polymer forms irregularly shaped nanometer-sized domains with sizes around 50–60 nm.

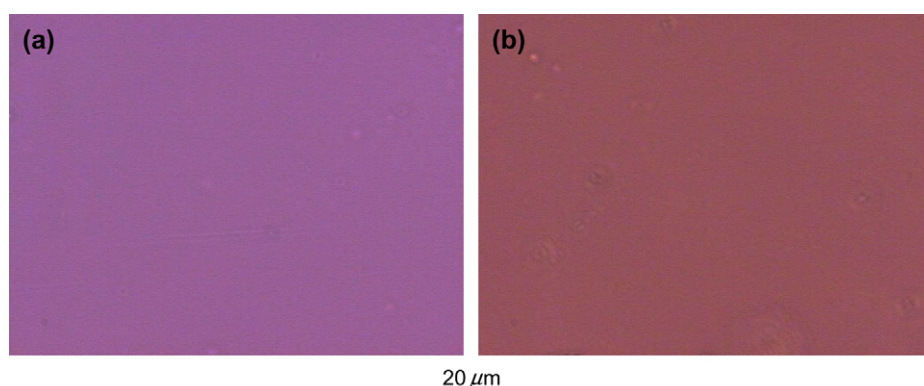


Fig. 2. PLM observation of: (a) Torlon/Matrimid (1:1) and (b) Torlon/PBI (1:1) blend films.

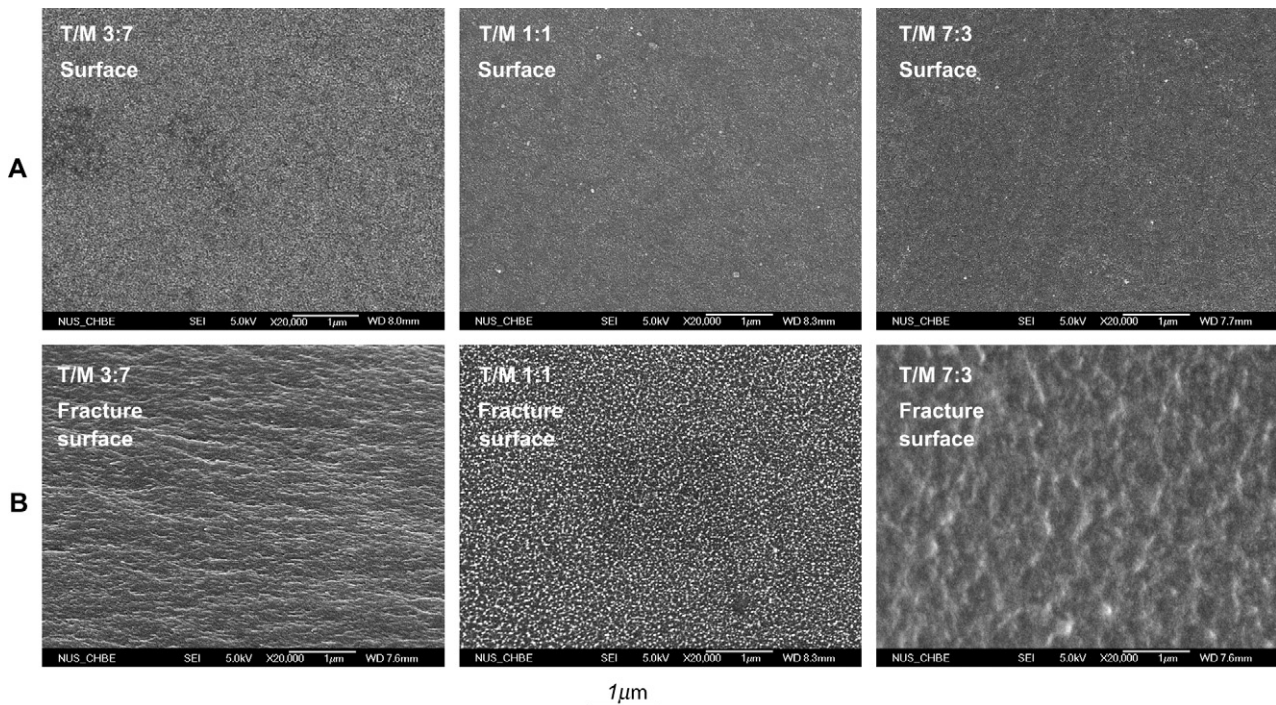


Fig. 3. FESEM micrographs of: (A) the surface and (B) fracture surface of Torlon/Matrimid blend films at different compositions.

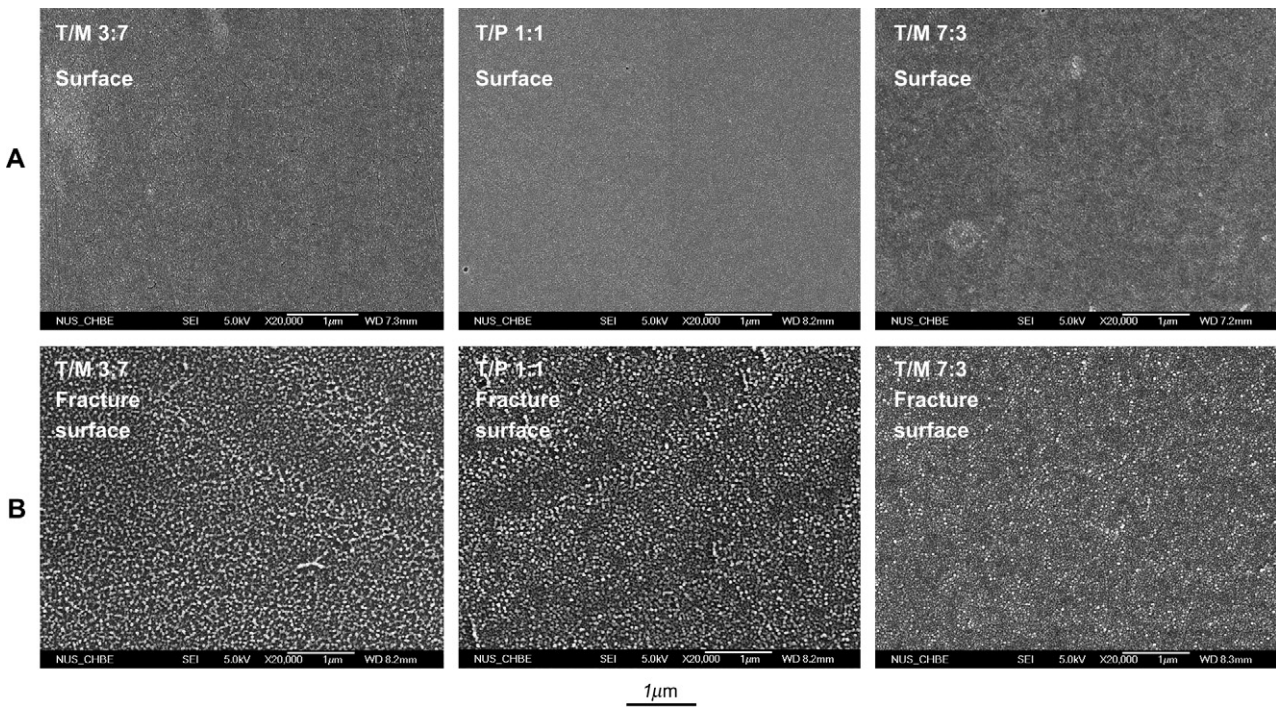


Fig. 4. FESEM micrographs of: (A) the surface and (B) fracture surface of Torlon/PBI blend films at different compositions.

### 3.2. Glass transition temperature of the polymer blends

The most commonly used criterion for miscibility is the existence of a single  $T_g$  intermediate to those of the two pure components.  $T_g$  can be measured by calorimetric determination of heat capacities as a function of temperature and also by dynamic mechanical measurement of complex modulus

as a function of temperature. Due to the availability of relatively inexpensive equipment and ease of operation, differential scanning calorimetry (DSC) is the most popular method for  $T_g$  measurement.

DSC results show the existence of a single  $T_g$  over the whole composition range for each Torlon/Matrimid and Torlon/PBI blend, indicating that miscibility exists over the

whole composition range for these two blend systems. The DSC curves of the two blend systems obtained from modulated DSC are shown in Figs. 5 and 6, respectively. A single well-defined glass transition can be observed for each blend.

The  $T_g$ -composition curves of the two blend systems are shown in Figs. 7 and 8. The  $T_g$ -composition curve of the Torlon/Matrimid blend system forms a sigmoid curve as a function of composition. At low Torlon contents, the  $T_g$  values are higher than the weighted-average value based on the linear additivity rule, whereas at high Torlon contents, the  $T_g$  values are lower than the weighted-average values. The  $T_g$ -composition curve of the Torlon/PBI blend system is double parabola-like. These double parabola-like curves have also been reported in some other polymer blended systems [50,51]. However, in most situations the parabola in the  $T_g$ -composition curve shows upward convexity.

S-shaped  $T_g$ -composition curves of miscible polymer blend systems are generally fitted using the Kwei equation:

$$T_g = \frac{w_1 T_{g1} + k w_2 T_{g2}}{w_1 + k w_2} + q w_1 w_2$$

where  $w_i$  and  $T_{gi}$  are the weight fraction and  $T_g$  of polymer  $i$ , and  $k$  and  $q$  are fitting constants.

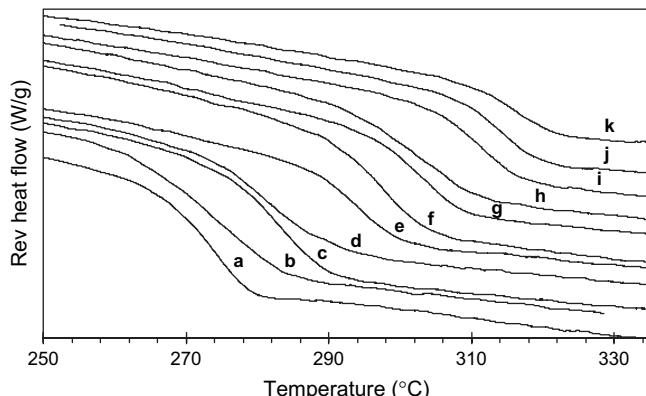


Fig. 5. DSC curves of the Torlon/Matrimid blend system obtained from modulated DSC containing: (a) 100, (b) 90, (c) 80, (d) 70, (e) 60, (f) 50, (g) 40, (h) 30, (i) 20, (j) 10 and (k) 0 wt% Torlon.

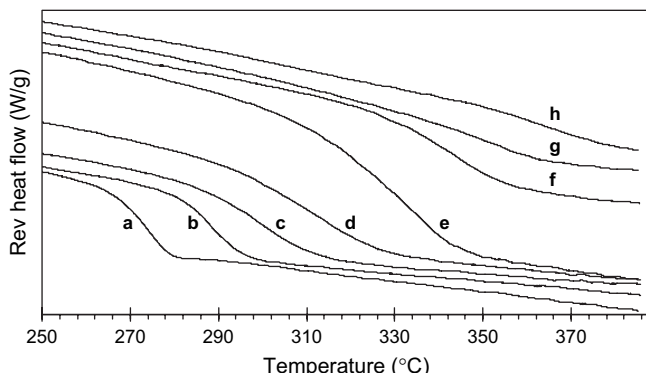


Fig. 6. DSC curves of the Torlon/PBI blend system obtained from modulated DSC containing: (a) 100, (b) 90, (c) 80, (d) 70, (e) 60, (f) 50, (g) 40 and (h) 30 wt% Torlon.

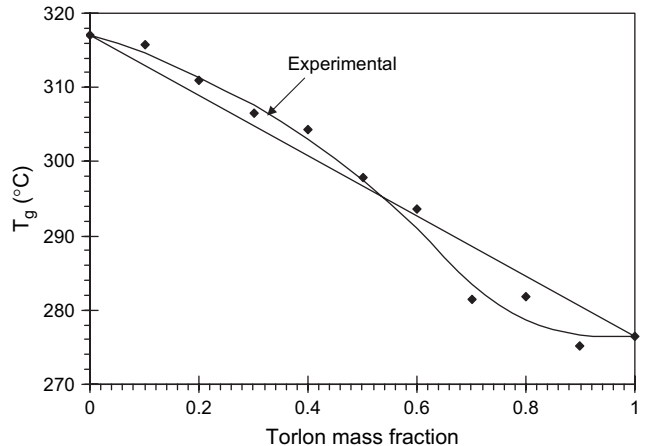


Fig. 7.  $T_g$ -composition curve of the Torlon/Matrimid blend system.

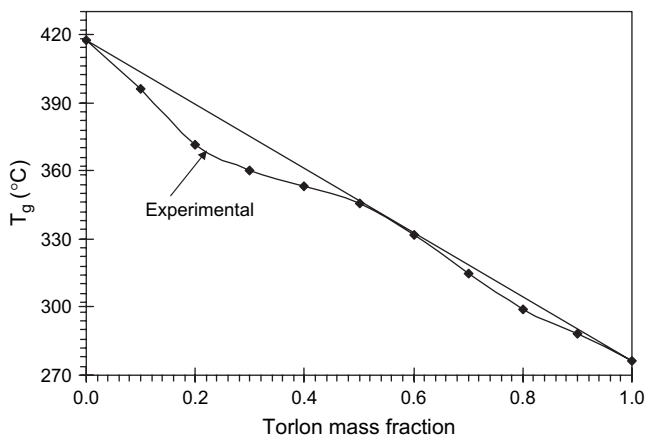


Fig. 8.  $T_g$ -composition curve of the Torlon/PBI blend system.

We have tried to simulate the  $T_g$ -composition curves using the Kwei equation but without success. We examined several polymer blend systems with S-shaped  $T_g$ -composition curves [51–56] which can be fitted by the Kwei equation. For those blend systems, blends rich in high- $T_g$  component showed negative deviations in the  $T_g$  values, whereas blends rich in low- $T_g$  component showed positive deviations in the  $T_g$  values. The  $T_g$  behavior of the Torlon/Matrimid blend system is different. Blends rich in Matrimid (the high- $T_g$  component) showed positive deviations in the  $T_g$  values and blends rich in Torlon (the low- $T_g$  component) showed negative deviations. Not many miscible blend systems showed  $T_g$  behavior similar to the Matrimid/Torlon system [17,57], and the  $T_g$ -composition curves could not be fitted by the Kwei equation. There was one report [58] using the Kwei equation to fit this kind of S-shaped  $T_g$ -composition curve. However, we found that the given  $k$  and  $q$  values could not fit that  $T_g$ -composition curve.

Modulated DSC, a newly developed technique, was used in this study to determine the glass transitions of the two blend systems. In a conventional DSC ramp, the temperature changes linearly with time. However, in MDSC, a sinusoidal modulation (oscillation) is overlaid on the conventional linear heating or cooling ramp to yield a profile in which the average

sample temperature changes continuously but not in a linear fashion. Thus under the modulated-temperature mode the sample is remained in a quasi-equilibrium state. The  $T_g$  determined by MDSC using this program is therefore more reliable, and used to plot the  $T_g$ -composition curves. However, for the Torlon/PBI blend system,  $T_g$  could not be detected when PBI content is higher than 70 wt% because the neat PBI has a high  $T_g$  of 417.1 °C, which is beyond the MDSC maximum testing temperature (i.e., 385 °C). Thus we take the conventional DSC results for the  $T_g$ -composition curve when the PBI content is greater than 70 wt%.

Tables 1 and 2 give the  $T_g$  values obtained from conventional DSC, MDSC and DMA. Generally the  $T_g$  values from DMA (to be discussed later) are higher as compared to the corresponding values from DSC.

To further confirm that these two blend systems are miscible systems thermodynamically, the blend samples were annealed for 10 min at various temperatures, quench cooled to 50 °C and rescanned. For the Torlon/Matrimid system, the annealing temperatures were 280, 300, 320 and 340 °C. For the Torlon/PBI system, the annealing temperatures were 280, 340, 380 and 400 °C. A single  $T_g$  was observed for all the annealed samples, showing that annealing did not lead to phase separation. Therefore, both the Torlon/Matrimid and Torlon/PBI blend systems are miscible thermodynamically.

Table 1  
 $T_g$  values of the Torlon/Matrimid blend systems obtained from conventional DSC, MDSC and DMA

	Conventional DSC (°C)	Modulated DSC (°C)	DMA (°C)	
			Loss modulus	Tan δ
Matrimid	320.8	317.0	324.34	335.3
T/M 1:9	316.3	315.5	319.71	334.4
T/M 2:8	314.3	310.9	—	—
T/M 3:7	311.7	306.6	314.99	322.3
T/M 4:6	304.1	304.4	—	—
T/M 1:1	304.1	297.9	307.37	317.7
T/M 6:4	297.6	294.1	—	—
T/M 7:3	292.8	280.3	299.37	308.8
T/M 8:2	288.8	283.0	—	—
T/M 9:1	280.7	273.1	286.50	297.8
Torlon	274.7	276.4	281.54	291.6

Table 2  
 $T_g$  values of the Torlon/PBI blend systems obtained from conventional DSC, MDSC and DMA

	Conventional DSC (°C)	Modulated DSC (°C)	DMA (°C)	
			Loss modulus	Tan δ
PBI	417.1	—	—	—
T/P 1:9	396.2	—	395.67	431.3
T/P 2:8	371.6	—	—	—
T/P 3:7	342.0	367.7	373.91	408.6
T/P 4:6	327.0	355.0	—	—
T/P 1:1	327.0	345.3	354.83	377.4
T/P 6:4	318.8	331.6	—	—
T/P 7:3	313.2	314.5	326.76	347.8
T/P 8:2	305.6	299.1	—	—
T/P 9:1	299.1	288.1	298.49	312.9
Torlon	274.7	276.4	281.54	291.6

### 3.3. FTIR characterization

The existence of hydrogen-bonding interaction in Torlon/Matrimid and Torlon/PBI blends has been investigated using FTIR. The FTIR spectra of Torlon/PBI and Torlon/Matrimid systems are shown in Figs. 9 and 10.

The FTIR spectrum of PBI is characterized by several typical peaks as reported by Musto et al. [17–22]. As shown in Fig. 11, the IR spectrum of PBI can be tentatively assigned as follows: the moderately strong peak 1 at around 3400  $\text{cm}^{-1}$  is due to “free” non-hydrogen-bonded N–H stretching; while the small shoulder peak at about 3145  $\text{cm}^{-1}$  can be assigned to the self-associated N–H stretching; the small peak 3 in the vicinity of 3050  $\text{cm}^{-1}$  arises from the aromatic C–H stretching; and another moderately strong peak 4 at 1620  $\text{cm}^{-1}$  is caused by the C=C and C=N stretching.

We shall look at the IR spectra of Torlon/PBI blend system first (Fig. 9). The self-associating N–H stretching peak (3145  $\text{cm}^{-1}$ ) of PBI moves to a high frequency, and then replaced by a large shoulder-like peak as the Torlon content increases, indicating a weakening of the self-association and the replacement by a hydrogen bonding between PBI and Torlon.

We can further look at the locally enlarged spectra in the region of 1760–1620  $\text{cm}^{-1}$  in Fig. 12 to see the influence of blending on the Torlon stretching peaks. There are two types of carbonyl groups in Torlon: the imide carbonyl which absorbs at 1720  $\text{cm}^{-1}$  and the amide carbonyl which absorbs at around 1645  $\text{cm}^{-1}$ . As shown in Fig. 12, the imide carbonyl band is more intense than the amide carbonyl band. PBI does not absorb in that region as it does not possess carbonyl groups. As PBI is added to Torlon, the intensity ratio of the 1720  $\text{cm}^{-1}$  band to 1645  $\text{cm}^{-1}$  band decreases. The change in the intensity ratio suggests that the interaction between Torlon and PBI is through hydrogen bonding between the imide carbonyl of Torlon and the N–H group of PBI, and the hydrogen-bonded imide carbonyl band happens to absorb at about the same frequency as the amide carbonyl band. As a result, the intensity of the 1645  $\text{cm}^{-1}$  band increases with increasing PBI content.

The IR spectra of the Torlon/Matrimid blend system as shown in Figs. 10 and 13 are more complicated. There are two possibilities of interactions between Matrimid and Torlon. One is the charge transfer interactions as reported by Hasegawa et al. [23,24,31] for some polyimide blends. The charge transfer interactions between the imide group and the *p*-phenylene group of PIs may happen between the same polymer molecules (Torlon or Matrimid), or between Torlon and Matrimid molecules. It is believed that the interaction between Torlon and Matrimid molecules is stronger than the one between the same polymer molecules. The other possibility is the hydrogen bonding between Torlon N–H group and Matrimid imide carbonyl group. We try to analyze the FTIR spectra as shown in Figs. 10 and 13. Fig. 13 shows the locally enlarged FTIR spectra in the 1760–1630  $\text{cm}^{-1}$  region. Matrimid possesses both an imide carbonyl band and a benzophenone carbonyl band at 1670  $\text{cm}^{-1}$ , which are close to the amide carbonyl band of Torlon. As a result, the spectra of various

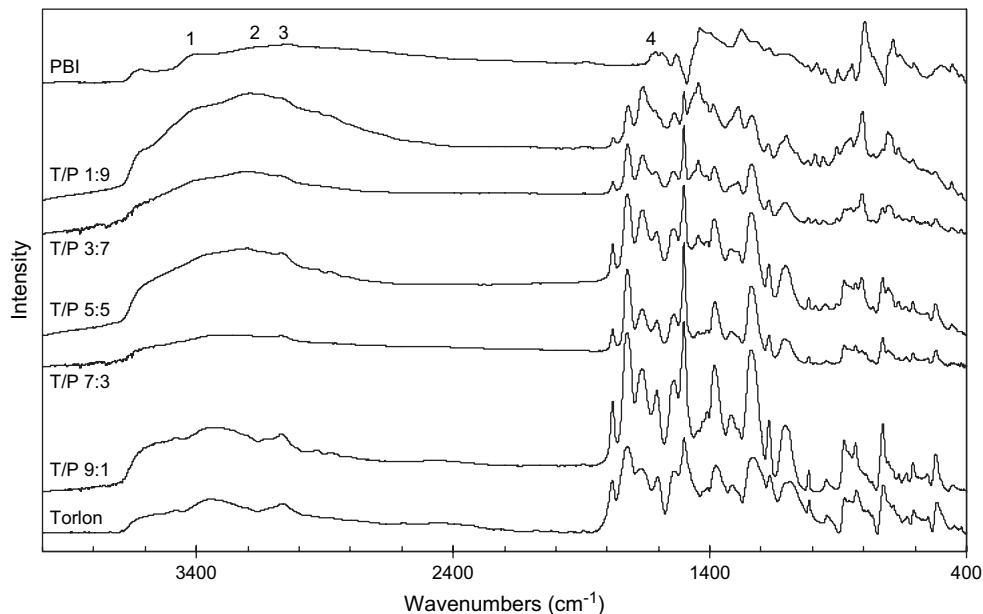


Fig. 9. FTIR spectra of the Torlon/PBI blend system.

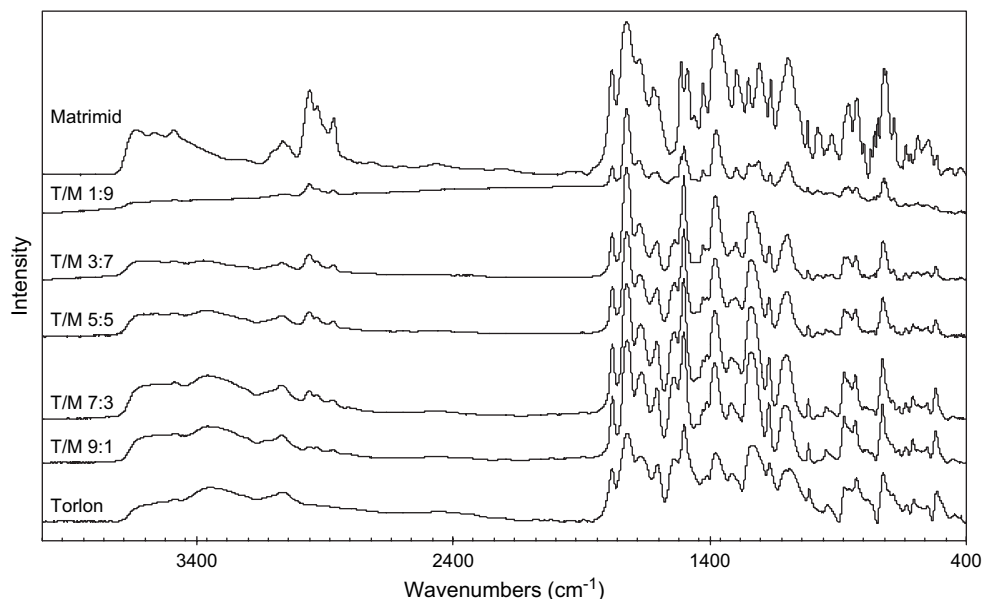


Fig. 10. FTIR spectra of the Torlon/Matrimid blend system.

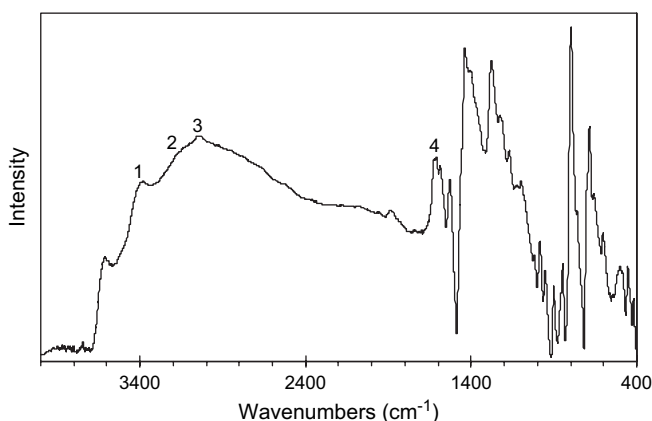


Fig. 11. FTIR spectrum of pure PBI.

Torlon/Matrimid blends are quite similar. On a closer look, it appears that the maximum of the carbonyl band in the  $1670\text{ cm}^{-1}$  region shifts slightly to a lower frequency upon the addition of Torlon. This may be caused by the hydrogen-bonding interaction between these two polymer molecules.

### 3.4. DMA characterization

Fig. 14 illustrates the  $\tan \delta$  curves of the two blend systems. The  $\alpha$  transition is the glass transition which is associated with the relaxation of the main backbone chain and was determined by the  $\tan \delta$  peak. For the two blend systems, each blend shows a single  $T_g$ , which decreases with an increase in Torlon content. Tables 1 and 2 summarize the glass transition

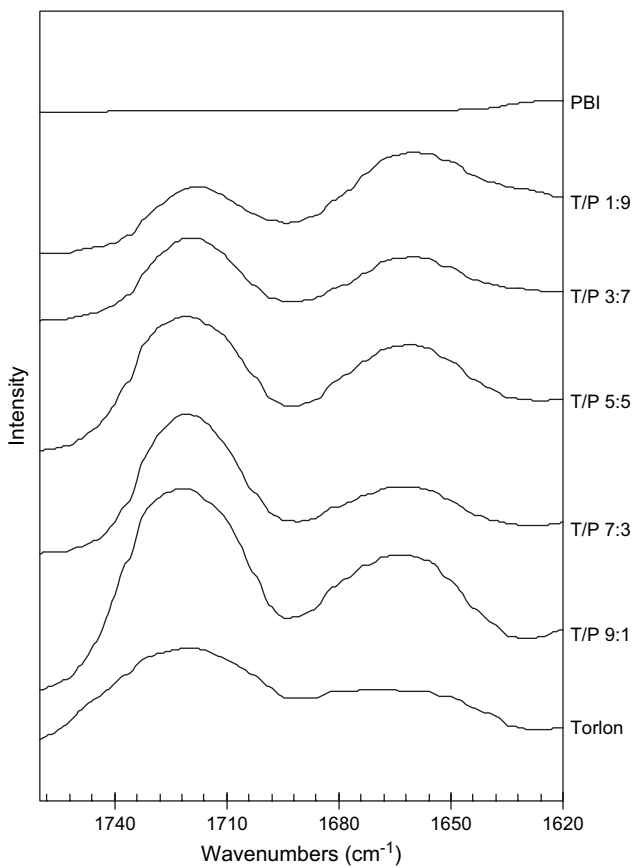


Fig. 12. FTIR spectra in the 1760–1620  $\text{cm}^{-1}$  region of the Torlon/PBI blend system.

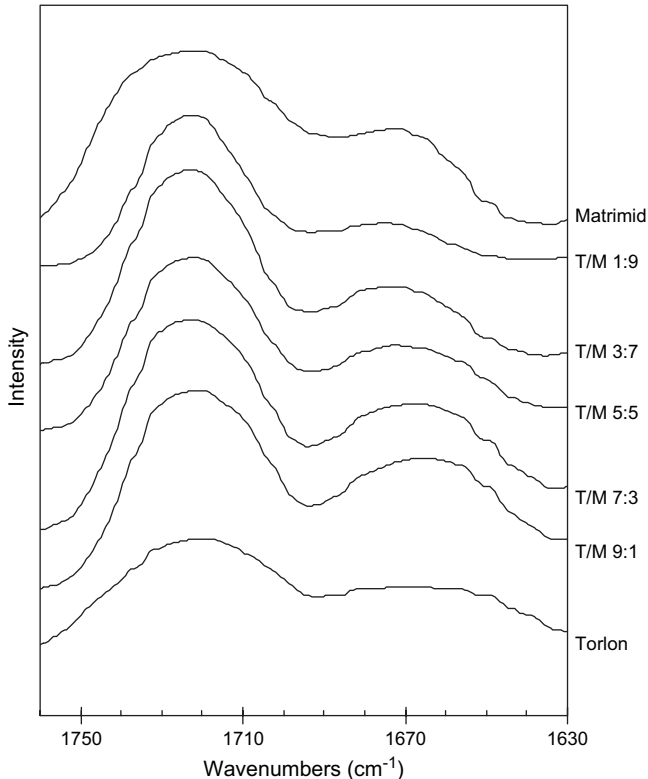


Fig. 13. FTIR spectra in the 1760–1630  $\text{cm}^{-1}$  region of the Torlon/Matrimid blend system.

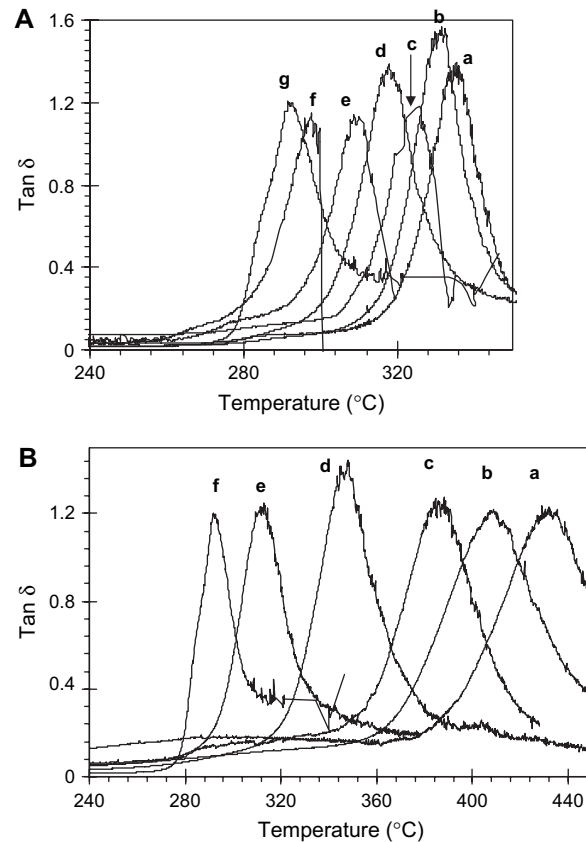


Fig. 14. (A)  $\tan \delta$  curves of Torlon/Matrimid blend containing: (a) 0, (b) 10, (c) 30, (d) 50, (e) 70, (f) 90 and (g) 100 wt% Torlon. (B)  $\tan \delta$  curves of the Torlon/PBI blend containing: (a) 10, (b) 30, (c) 50, (d) 70, (e) 90 and (f) 100 wt% Torlon.

temperatures obtained from conventional DSC, MDSC and DMA.  $T_g$  obtained from  $\tan \delta$  and loss modulus spectra are both given. The  $T_g$  values obtained from DMA are higher than the corresponding values from DSC, while the values from  $\tan \delta$  spectra are still higher than those from the loss modulus spectra. Both DSC and DMA results confirm the miscibility of Torlon with either Matrimid or PBI.

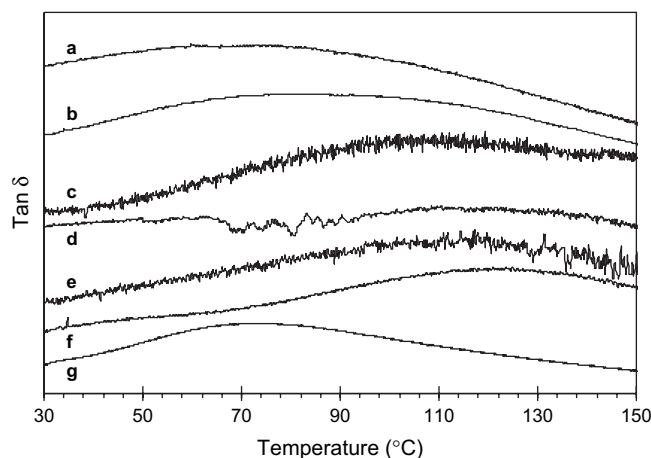


Fig. 15.  $T_\beta$  shift in the  $\tan \delta$  curves of Torlon/Matrimid blend systems with (a) 0, (b) 10, (c) 30, (d) 50, (e) 70, (f) 90 and (g) 100 wt% Torlon content.

Fig. 15 illustrates the shift of  $T_\beta$  of the Torlon/Matrimid blend with different compositions. The  $T_\beta$  shifts to higher temperature when the Torlon content is increased. Torlon/Matrimid (9:1) blend has a highest  $T_\beta$ , which is higher than both neat polymers. Because the rotation of benzene rings and cooperative motion of these rings within a small localized scale correspond to the  $\beta$  transition in the  $\tan \delta$  curve of the polymer, a higher  $T_\beta$  suggests that the rotation of benzene rings becomes more difficult. This phenomenon is easy to explain. The existence of interactions between the polymer chains of Torlon and Matrimid may give more hindrance to the rotation of benzene rings. This means that the hindrance induced by the interactions of Torlon and Matrimid's inter-molecular chains is stronger than that caused by the interactions of intra-molecular polymer chains.

#### 4. Conclusions

We have found that miscibility exists in two blend systems of Torlon/Matrimid and Torlon/PBI over the whole composition range as confirmed by microscopy, DSC, modulated DSC, and DMA. The  $T_g$ -composition curve of the Torlon/Matrimid blend system is a sigmoid shape, while the  $T_g$ -composition curve of the Torlon/PBI blend system is a double parabola-like shape. FTIR spectra show the existence of hydrogen bonding in these two blend systems.

#### Acknowledgements

Financial supports from the National University of Singapore (NUS) under the research grants R-279-000-165-112, R-279-000-184-112 and R-279-000-008-001 are gratefully acknowledged. Thanks are also due to Ms. S.M. Tang, and Mr. L. Wang from Institute of Material Research and Engineering (IMRE) for their kind help for the use of DMA and FTIR. Special thanks are given to Solvay Advanced Polymers for the provision of free Torlon polymer samples.

#### References

- [1] Mark JE, editor. *Polymer data handbook*. New York: Oxford University Press; 1999. p. 260.
- [2] Robertson GP, Guiver MD, Yoshikawa M, Brownstein S. *Polymer* 2004;45:1111.
- [3] Yoshikawa M, Higuchi A, Ishikawa M, Guiver MD, Robertson GP. *J Membr Sci* 2004;243:89.
- [4] Higuchi A, Yoshikawa M, Guiver MD, Robertson GP. *Sep Sci Technol* 2005;40:2697.
- [5] Takegami S, Tujii S, Yamada H. *Nippon Kagaku Kaishi* 1993;2:194.
- [6] Karcha RJ, Porter RS. *J Polym Sci Part B Polym Phys* 1993;31:821.
- [7] Karcha RJ, Porter RS. *Polymer* 1992;33:4866.
- [8] Karcha RJ, Porter RS. *J Polym Sci Part B Polym Phys* 1989;27:2153.
- [9] Palsule S, Cowie JMG. *Polym Bull* 1994;33:241.
- [10] Wang JT, Savinell RF, Wainright J, Litt M, Yu H. *Electrochim Acta* 1996;41:191.
- [11] Bouchet R, Siebert E, Vitter G. *J Electrochem Soc* 1997;144:L95.
- [12] Pu HT, Liu QZ, Qiao L, Yang ZL. *Polym Eng Sci* 2005;45:1395.
- [13] Daletou MK, Gourdoupi N, Kallitsis JK. *J Membr Sci* 2005;252:115.
- [14] Wycisk R, Lee JK, Pintauro PN. *J Electrochem Soc* 2005;152:A892.
- [15] Chung TS, Guo WF, Liu Y. *J Membr Sci* 2006;271:221.
- [16] Cha YJ, Kim ET, Ahn TK, Choe S. *Polym J* 1994;26:1227.
- [17] Foldes E, Fekete E, Karasz FE, Pukanszky B. *Polymer* 2000;41:975.
- [18] Guerra G, Choe S, Williams DJ, Karasz FE, Macknight WJ. *Macromolecules* 1988;21:231.
- [19] Musto P, Karasz FE, MacKnight WJ. *Macromolecules* 1991;24:4762.
- [20] Ahn TK, Kim M, Choe S. *Macromolecules* 1997;30:3369.
- [21] Musto P, Karasz FE, MacKnight WJ. *Polymer* 1993;34:2934.
- [22] Musto P, Karasz FE, MacKnight WJ. *Polymer* 1989;30:1012.
- [23] Hasegawa M, Mita I, Kochi M, Yokota R. *Polymer* 1991;32:3225.
- [24] Hasegawa M, Ishii J, Shindo Y. *Macromolecules* 1999;32:6111.
- [25] Hasegawa M, Okuda K, Horimoto M, Shindo Y, Yokota R, Kochi M. *Macromolecules* 1997;30:5745.
- [26] Campbell JA, Goodwin AA, Mercer FW, Reddy V. *High Perform Polym* 1997;9:263.
- [27] Han BJ, Park JM, Gryte CC. *Polym Eng Sci* 1993;33:901.
- [28] Zhang P, Sun ZH, Li G, Zhuang YG, Ding MX, Feng ZL. *Macromol Chem Phys* 1993;94:1871.
- [29] Goodwin AA. *J Appl Polym Sci* 1999;2:543.
- [30] Ryu CH, Kim YH, Bae YC. *Eur Polym J* 2000;36:495.
- [31] Tang H, Dong LS, Zhang J, Ding MX, Feng ZL. *Macromol Chem Phys* 1996;191:543.
- [32] Staudt-Bickel C, Koros WJ. *J Membr Sci* 1999;155:145.
- [33] Bos A, Punt IGM, Wessling M, Strathmann H. *J Polym Sci Part B Polym Phys* 1998;36:1547.
- [34] Clausi DT, Koros WJ. *J Membr Sci* 2000;167:79.
- [35] Burns RL, Koros WJ. *J Membr Sci* 2003;211:299.
- [36] Bos A, Punt I, Strathmann H, Wessling M. *AIChE J* 2001;47:1088.
- [37] Bos A, Punt IGM, Wessling M, Strathmann H. *Sep Purif Technol* 1998;14:27.
- [38] Wessling M, Lopez ML, Strathmann H. *Sep Purif Technol* 2001;24:223.
- [39] Xiao YC, Dai Y, Chung TS, Guiver MD. *Macromolecules* 2005;38:10042.
- [40] Xiao YC, Chung TS, Chng ML, Tarnai S, Yamaguchi A. *J Phys Chem B* 2005;109:18741.
- [41] Guo WF, Chung TS. *J Membr Sci* 2005;253:13.
- [42] Li DF, Chung TS, Wang R. *J Membr Sci* 2004;243:155.
- [43] Tin PS, Chung TS, Kawi S, Guiver MD. *Microporous Mesoporous Mater* 2004;73:151.
- [44] Jiang LY, Chung TS, Li DF, Cao C, Kulprathipanja A. *J Membr Sci* 2004;240:91.
- [45] Tin PS, Chung TS. *Macromol Rapid Commun* 2004;25:1247.
- [46] Tin PS, Chung TS, Liu Y, Wang R, Liu SL, Pramoda KP. *J Membr Sci* 2003;225:77.
- [47] Chung TS, Chan SS, Wang R, Lu ZH, He CB. *J Membr Sci* 2003;211:91.
- [48] Macheras JT, Bikson B, Nelson JK. US Patent 5,443,728; 1995.
- [49] Simmons JW, Ikiner OM. US Patent 5,232,472; 1993.
- [50] Cho J, Park MS, Cho JH, Ji BC, Han SS, Lyoo WS. *J Polym Sci Part B Polym Phys* 2001;39:1778.
- [51] Lin AA, Kwei TK, Reiser A. *Macromolecules* 1989;22:4112.
- [52] Coleman MM, Painter PC. *Prog Polym Sci* 1995;30:1.
- [53] Kwei TK, Pearce EM, Pennacchia JR, Charton M. *Macromolecules* 1987;20:1174.
- [54] Hsu WP. *J Appl Polym Sci* 2005;96:2064.
- [55] Kwei TK. *J Polym Sci Polym Lett Ed* 1984;22:307.
- [56] Pennacchia JR, Pearce EM, Kwei TK, Bulkin BJ, Chen JP. *Macromolecules* 1989;19:973.
- [57] Zhang Z, Mo Z, Zhang H, Zhang Y, Na T, An Y, et al. *J Polym Sci Part B Polym Phys* 2002;40:1957.
- [58] Urzua M, Gargallo L, Radic D. *J Appl Polym Sci* 2002;84:1245.